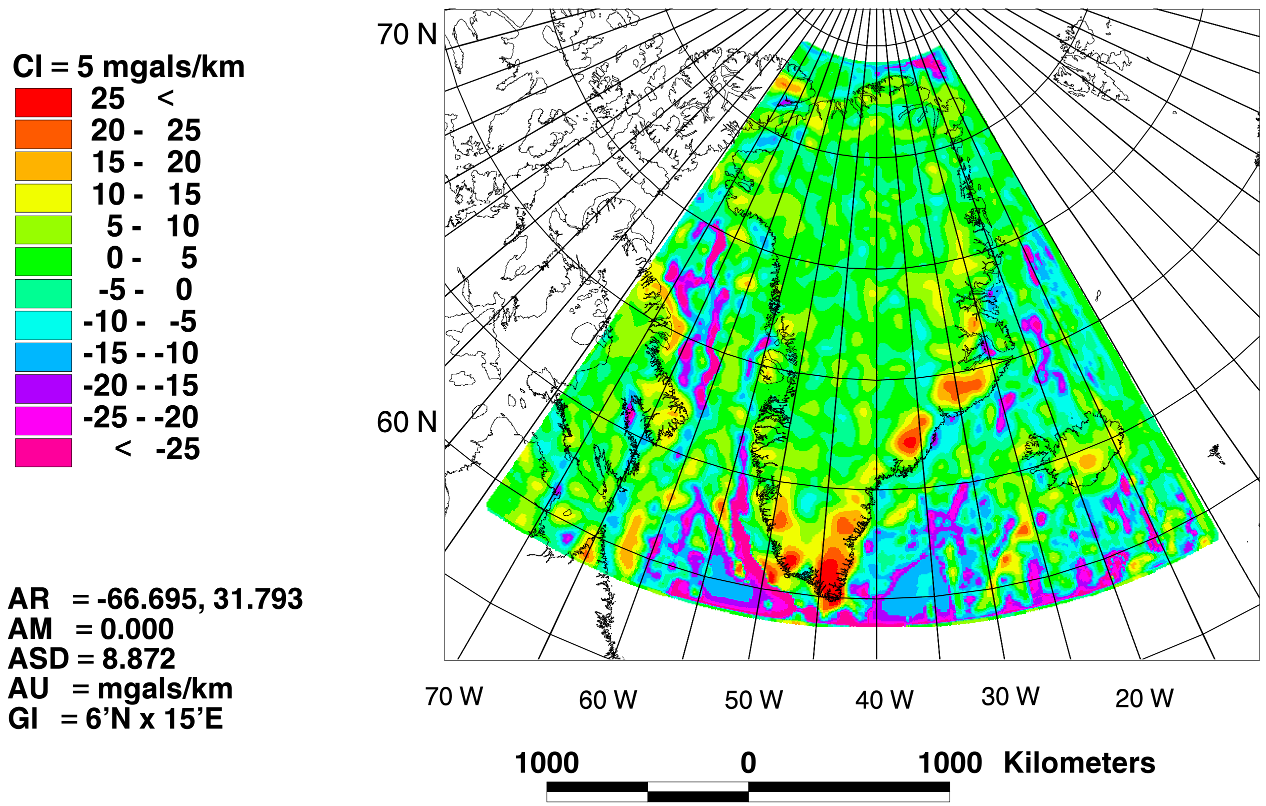

Figure 4.15: First vertical derivative of crustal gravity effect FVD(CGE) in a Lambert Equal-Area Azimuthal Projection centered on 40° W. These data were generated by applying a standard vertical derivative operator to the data in Figure 4.14.

Figure 4.12 and those wavenumbers that correlated at 0.39 and higher with the equivalent FVD(CGE) wavenumbers were passed. These passed wavenumbers represented the terrain-correlated component of the RTPMA shown in Figure 4.16 and demonstrated much higher (CC=0.40) correlation with the FVD(CGE) than the original RTPMA (CC=0.07) shown in Figure 4.12.

Removing the crustal thickness magnetic effects (Figure 4.16) from the RTPMA (Figure 4.12) yields residual anomalies of Figure 4.17 that may be taken to reflect intracrustal magnetic anomalies (i.e., IC-RTPMA). The IC-RTPMA tend to show enhanced relationships with regional geologic features of the study region, such as the prominent MA maxima associated with the volcanic rocks on Diskó Island or the MA minima over mantle rocks of the Iceland hotspot.

4.6 Gravity and Magnetic Anomaly Correlation Analysis

Correlations between gravity and magnetic anomalies provide powerful constraints for enhanced interpretation and quantitative analysis by joint inversion. To quantify possible correlations, Poisson's Relation (Equation 4.1) may be used to relate the IC-TDFAGA (Figure 4.7) and IC-RTPMA (Figure 4.17) through the first vertical derivative of IC-TDFAGA (i.e., FVD(IC-TDFAGA)) that is shown in Figure 4.18. IC-RTPMA and IC-TDFAGA were normalized to standard deviations of 10.0 [Davis, 1986; von Frese et al., 1997] as shown in Figures 4.19 and 4.20, respectively, to facilitate their graphical correlation by the relation:

$$N_i = (A_i - AM)NF^{-1} \tag{4.2}$$

where: N_i = normalized amplitude of anomaly
A_i = original amplitude of anomaly
AM = amplitude mean
$NF = \frac{10.0}{ASD}$ = normalization factor
ASD = amplitude standard deviation

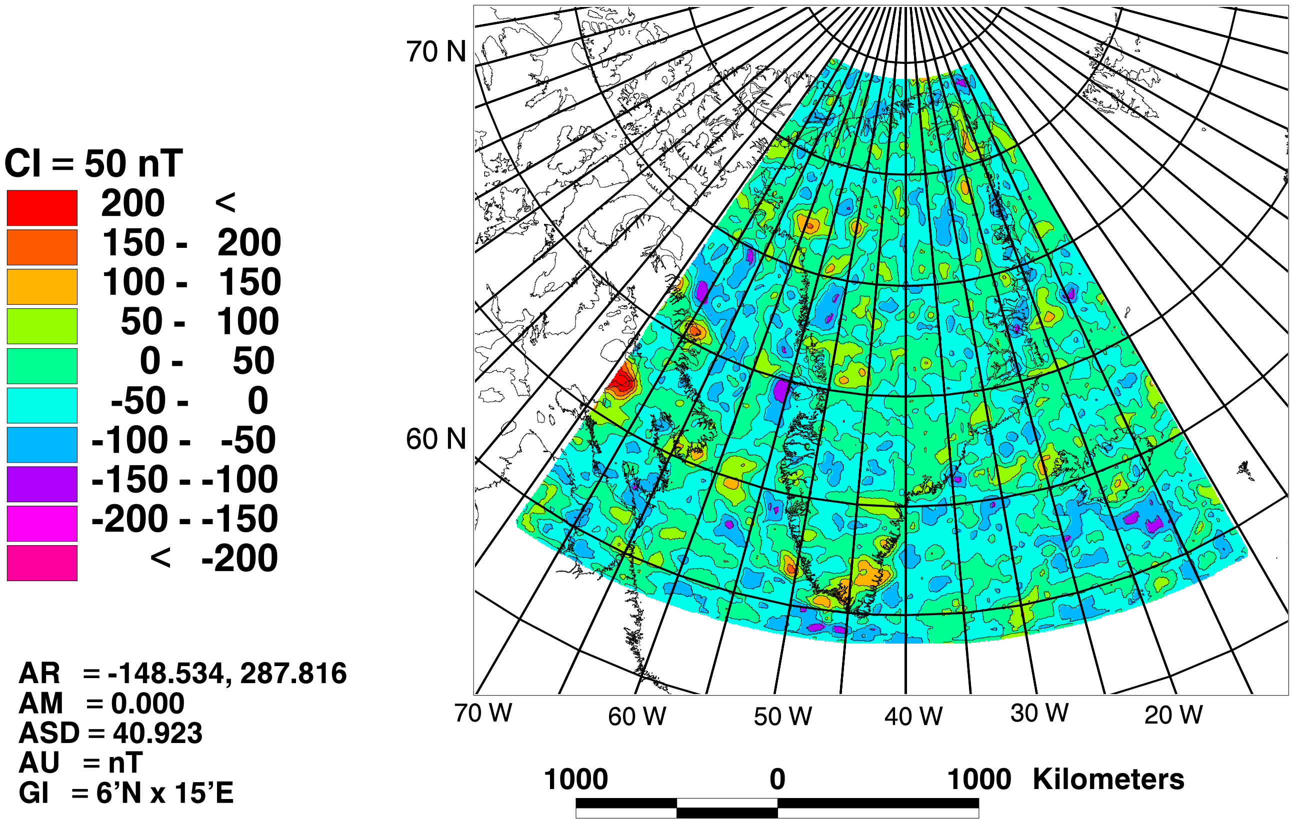

Figure 4.16: Crustal thickness MA that are the RTPMA components which are correlative with FVD(CGE) shown in Figure 4.15. Data are shown in a Lambert Equal-Area Azimuthal Projection centered on 40° W. These data were derived from wavenumber components of RTPMA in Figure 4.12 that correlated higher than 0.39 with the wavenumber components of FVD)CGE).

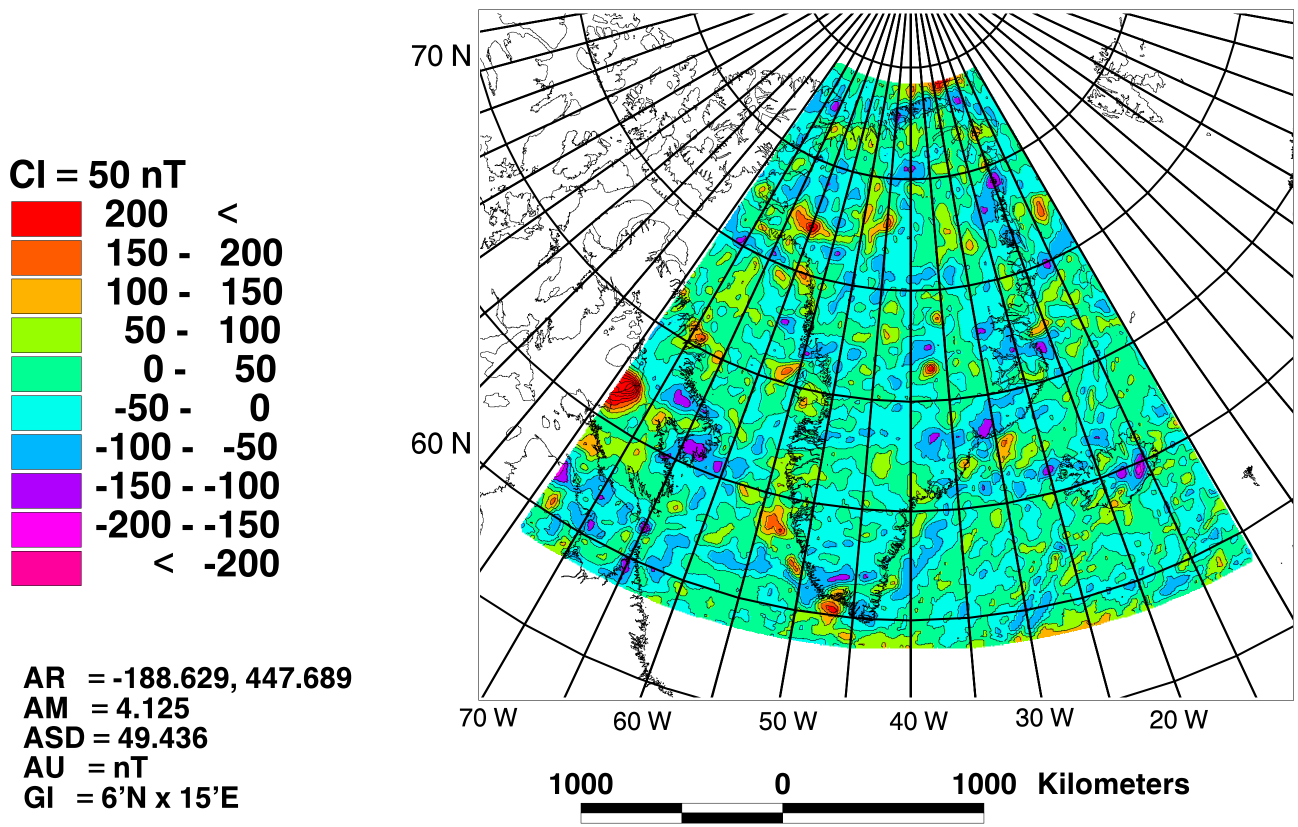

Figure 4.17: Intracrustal RTPMA (IC-RTPMA) in a Lambert Equal-Area Azimuthal Projection centered on 40° W.

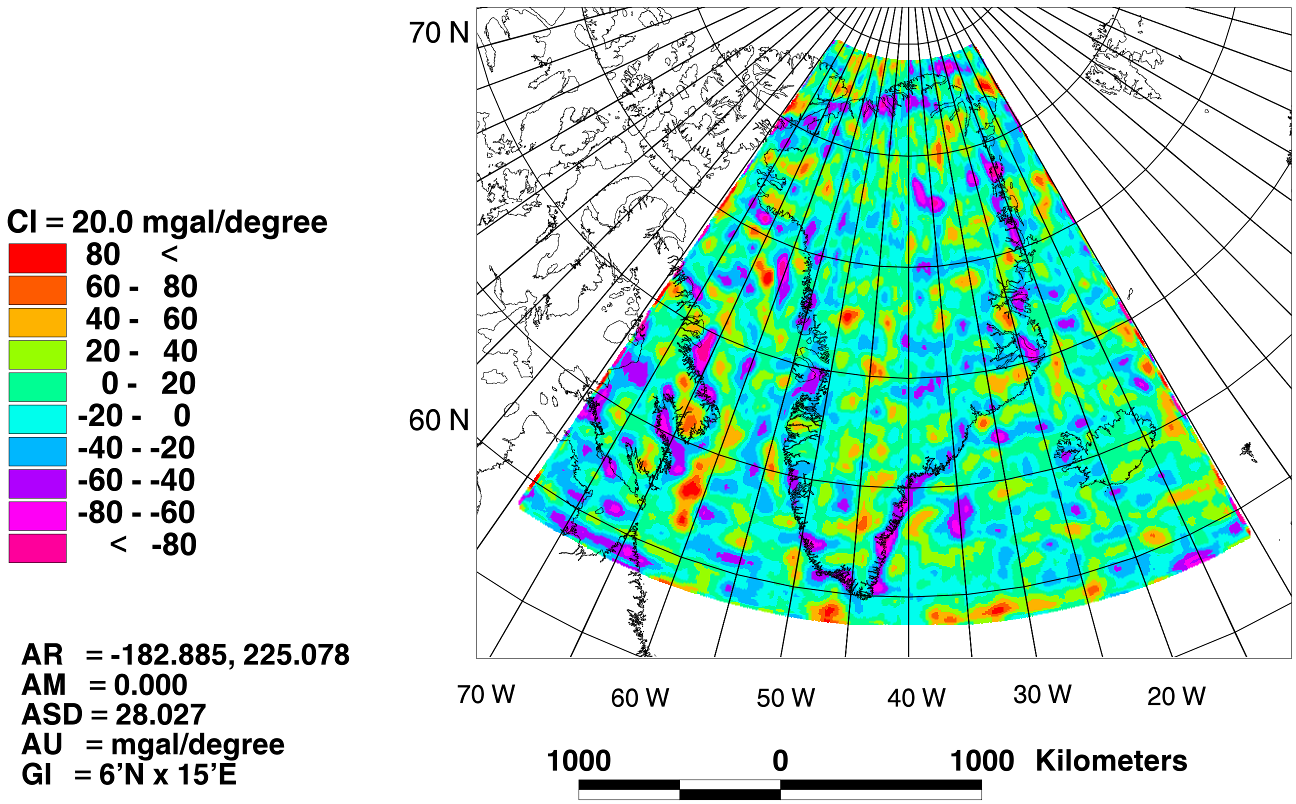

Figure 4.18: First vertical derivative terrain-decorrelated (FVD(IC-TDFAGA)) FAGA for Greenland in a Lambert Equal-Area Azimuthal Projection centered on 40° W. FVD(IC-TDFAGA) data are derived by taking the first radial derivative of the data shown in Figure 4.7.

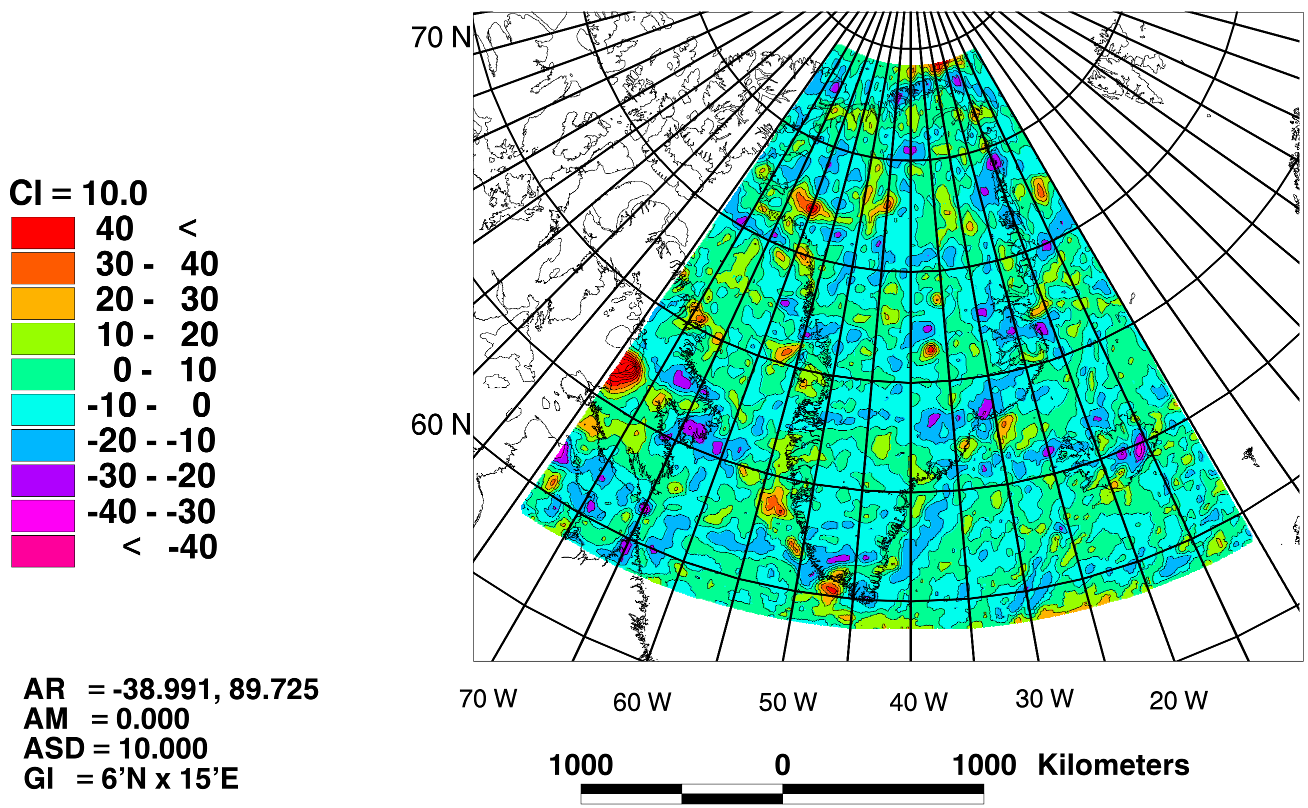

Figure 4.19: Normalized IC-RTPMA in a Lambert Equal-Area Azimuthal Projection centered on 40° W. Multiplying the normalized amplitudes by NF recovers the original amplitudes of the magnetic anomalies in Figure 4.17.

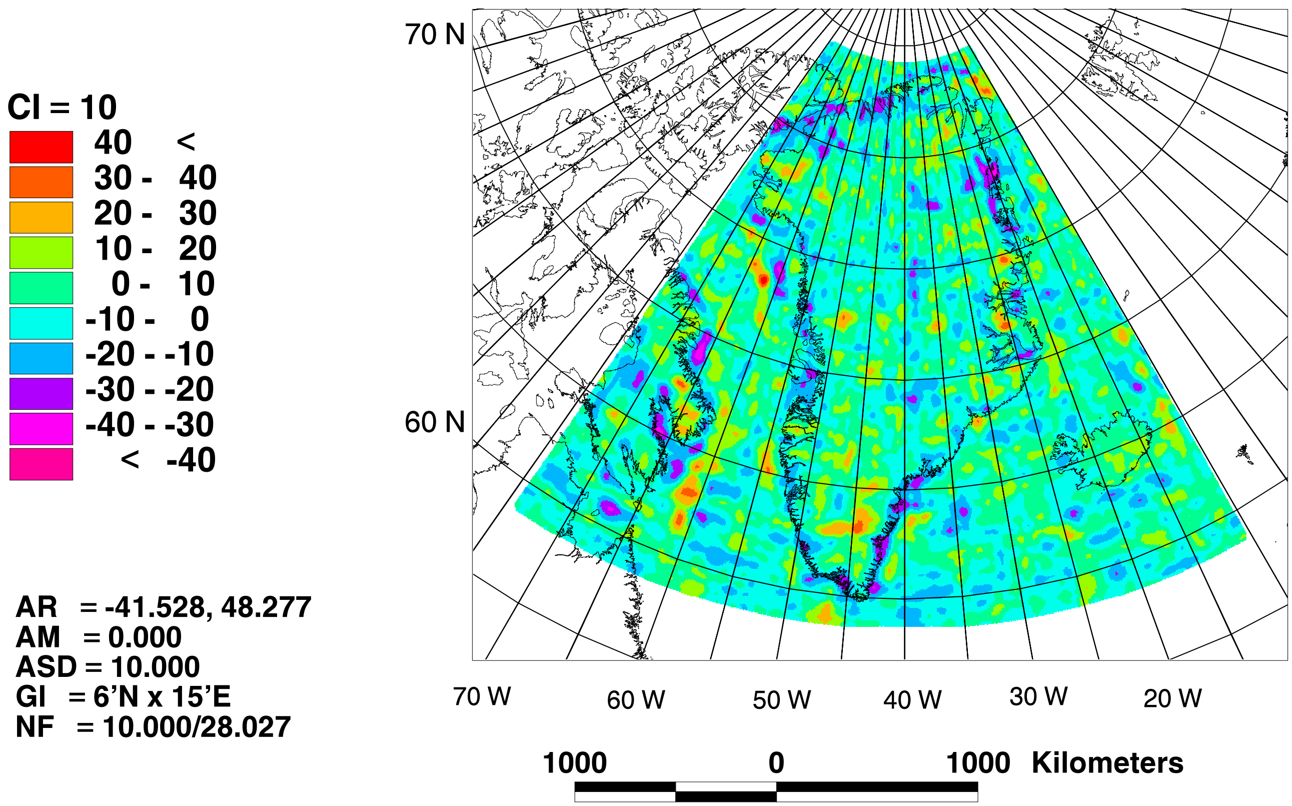

Figure 4.20: Normalized FVD(IC-TDFAGA) in a Lambert Equal-Area Azimuthal Projection centered on 40° W. Multiplying the normalized amplitudes by NF recovers the original amplitudes of the magnetic anomalies in Figure 4.7.

The normalized coefficients are dimensionless and unbiased, so that they may be added to generate the summed local favorability indices (SLFI) shown in Figure 4.21. SLFI > 0 highlight correlative gravity and magnetic maxima, whereas SLFI < 0 reflect correlative anomaly minima. The more prominent peak-to-peak and trough-to-trough associations are given by SLFI $>$ ASD(=10) and SLFI $<$ -ASD, respectively, which are shown in Figure 4.22.

The normalized coefficients may also be subtracted for differenced local favorability indices (DLFI) that highlight negatively correlated anomalies. Figure 4.23 gives the DLFI where the normalized IC-RTPMA (Figure 4.19) were subtracted from the normalized FVD(IC-TDFAGA) (Figure 4.20). DLFI > 0 tend to highlight gravity maxima that are correlative with magnetic minima, whereas DLFI < 0 reflect gravity minima that correlate with magnetic maxima. The more prominent gravity peak-to-magnetic trough and gravity trough-to-magnetic peak associations are given by DLFI $>$ ASD(=10) and DLFI $<$ -ASD, respectively, which are shown in Figure 4.24.

Null correlated features may be highlighted by taking the quotients of the normalized coefficients for quotient local favorability indices (QLFI). In evaluating the QLFIs, the absolute value of the denominator coefficients is taken to preserve the signs of the numerator coefficients. QLFI where the normalized gravity coefficients are in the numerator are called G-QLFI, whereas they are called M-QLFI when the normalized magnetic coefficients are in the numerator. Figure 4.25 shows G-QLFI > 1 in panel a and G-QLFI < -1 in panel b that reflect the distribution of gravity maxima and minima, respectively, which are not matched by positively or negatively correlative magnetic anomalies. On the other hand, Figure 4.26 gives the M-QLFI > 1 in panel a and M-QLFI < -1 in panel b that are not matched by correlative gravity anomalies.

This analysis has isolated prominent positively, negatively, and null correlated features in the intracrustal gravity and magnetic anomaly data of the Greenland study region. These associations and the geologic extents that they suggest are discussed briefly in the next section with an emphasis on the southwestern Greenland margin. The features highlighted by this process must be analyzed with care and alternative sources of information should be used to check the results whenever possible, because errors in the derivation of the favorability indices may originate from several sources. For example, the original data provided by GSC and NIMA contained significant errors in some of the areas (e.g., up to 100 nT and 15 mgals). These data were processed to remove terrain related effects, and hence terrain modeling errors can further contribute to the degradation in the data.

4.7 Discussion

Conspicuous patterns of correlative anomalies characterized the geologic features and provinces noted in Figures 4.22, 4.24, 4.25, and 4.26. These patterns were combined with the geologic structures implied by the Moho depth model in Figure 4.1 [Chapter 3] to develop improved insight on the distribution of these features beneath the region's ubiquitous cover of snow, ice and sea water.

Spectral correlation of FAGA and MA has been used here only to infer possible regional associations, because the physical properties of the rocks can have considerable variability even when derived from the same processes. Also because of this variability, combinations of Figures 4.22, 4.24, 4.25, and 4.26 may be necessary to account for variations of a lithology.

For example, the Nagssugtoqidian Province appears to be characterized internally by high to intermediate positive densities and strongly positive magnetic susceptibility contrasts as shown in Figures 4.22.a and 4.25.a. However, the northwestern and

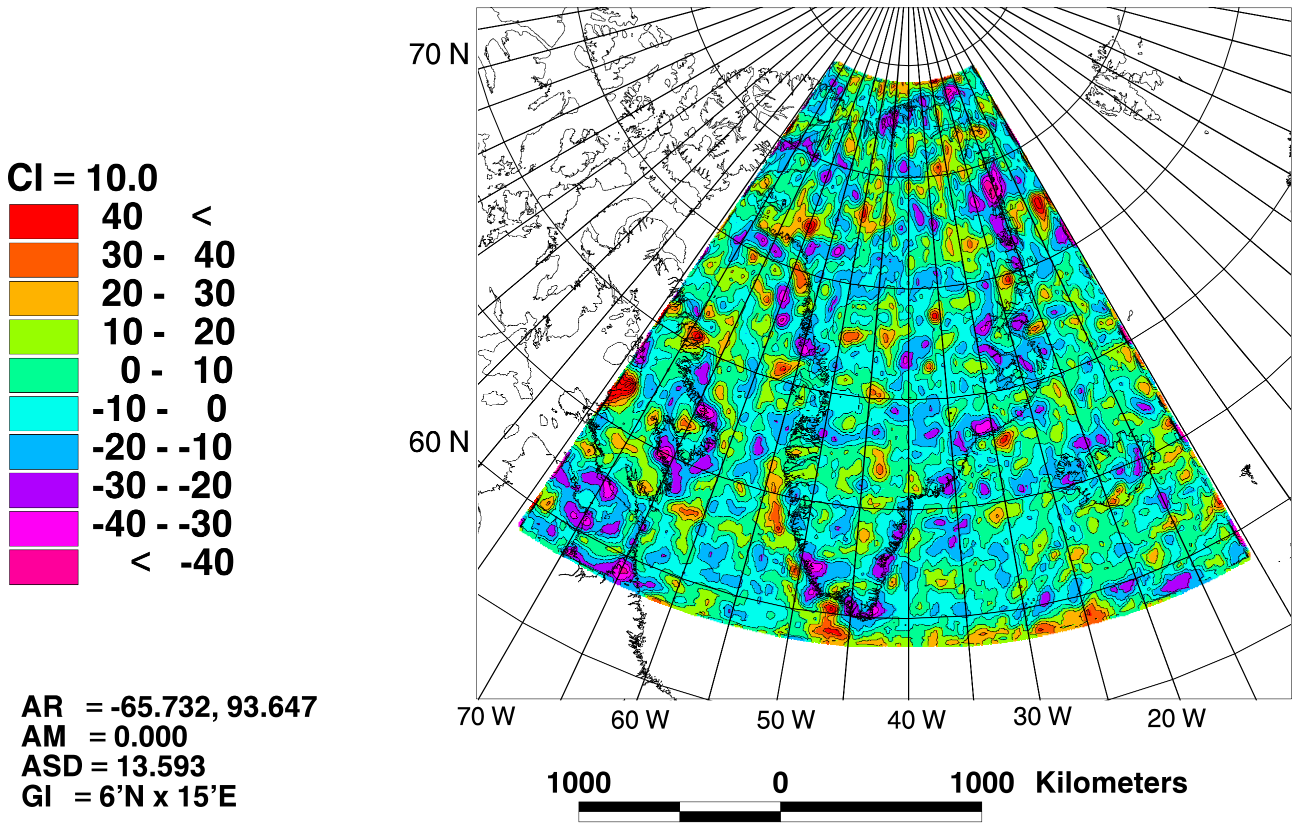

Figure 4.21: Summed local favorability indices (SLFI) from adding Figures 4.19 and 4.20 in a Lambert Equal-Area Azimuthal Projection centered on 40°W.

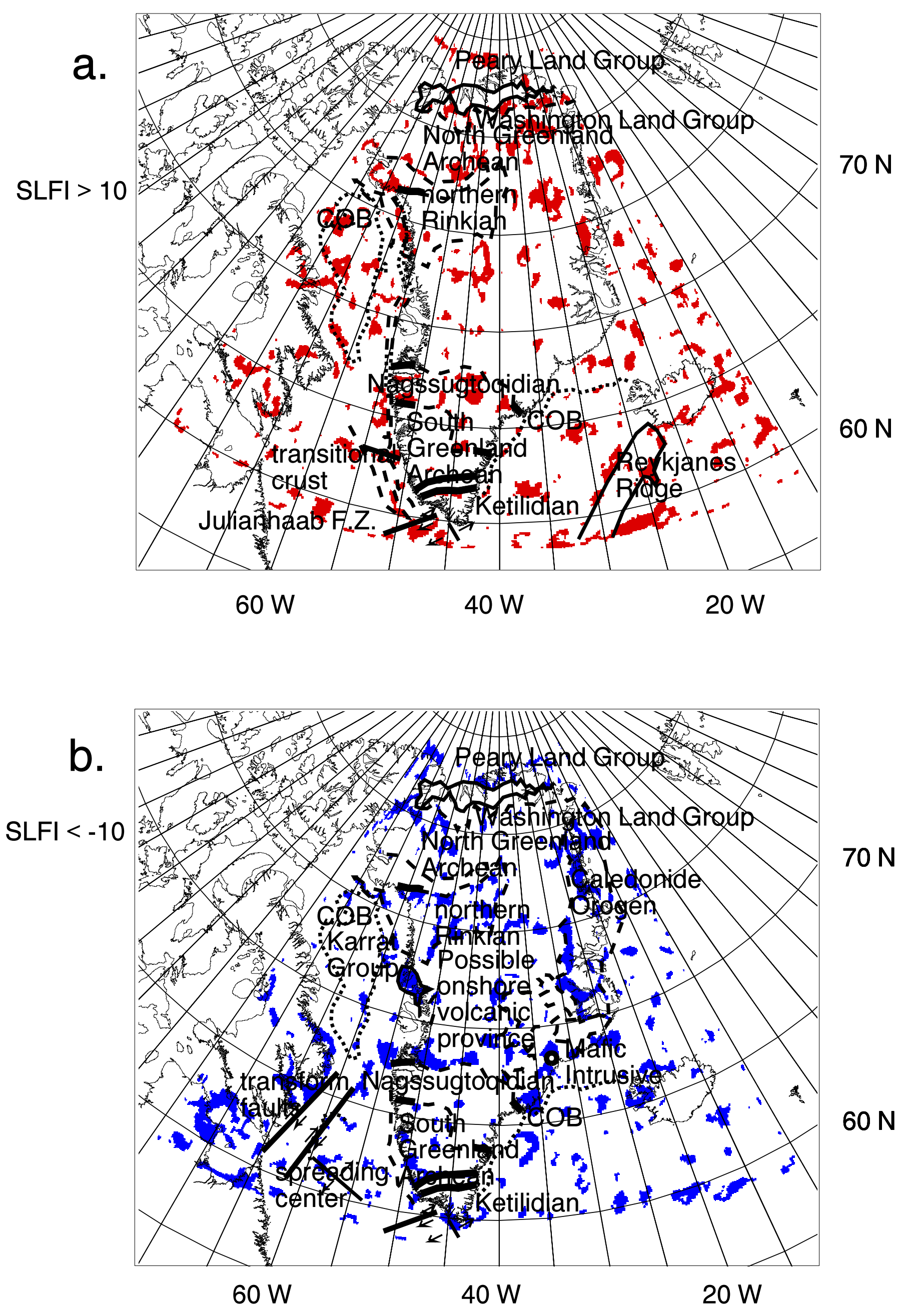

Figure 4.22: Positively correlated gravity and magnetic features for the Greenland study area in a Lambert Equal-Area Azimuthal Projection centered on 40° W. Noted features are discussed in the text. **a**) The stronger peak-to-peak correlations given by SLFI>ASD(=10). **b**) The stronger trough-to-trough correlations given by SLFI<-ASD.

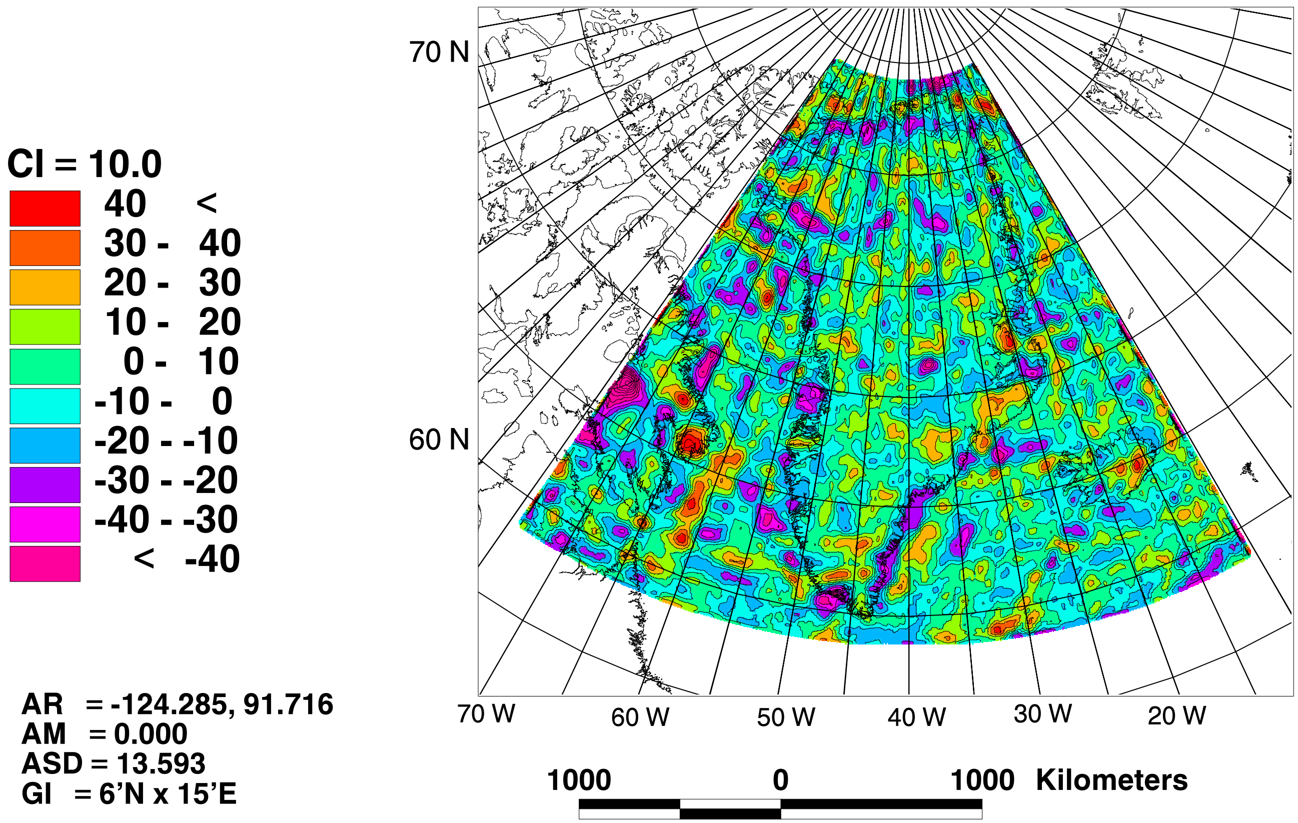

Figure 4.23: Differenced local favorability indices (DLFI) from subtracting Figures 4.19 and 4.20 in a Lambert Equal-Area Azimuthal Projection centered on 40° W.

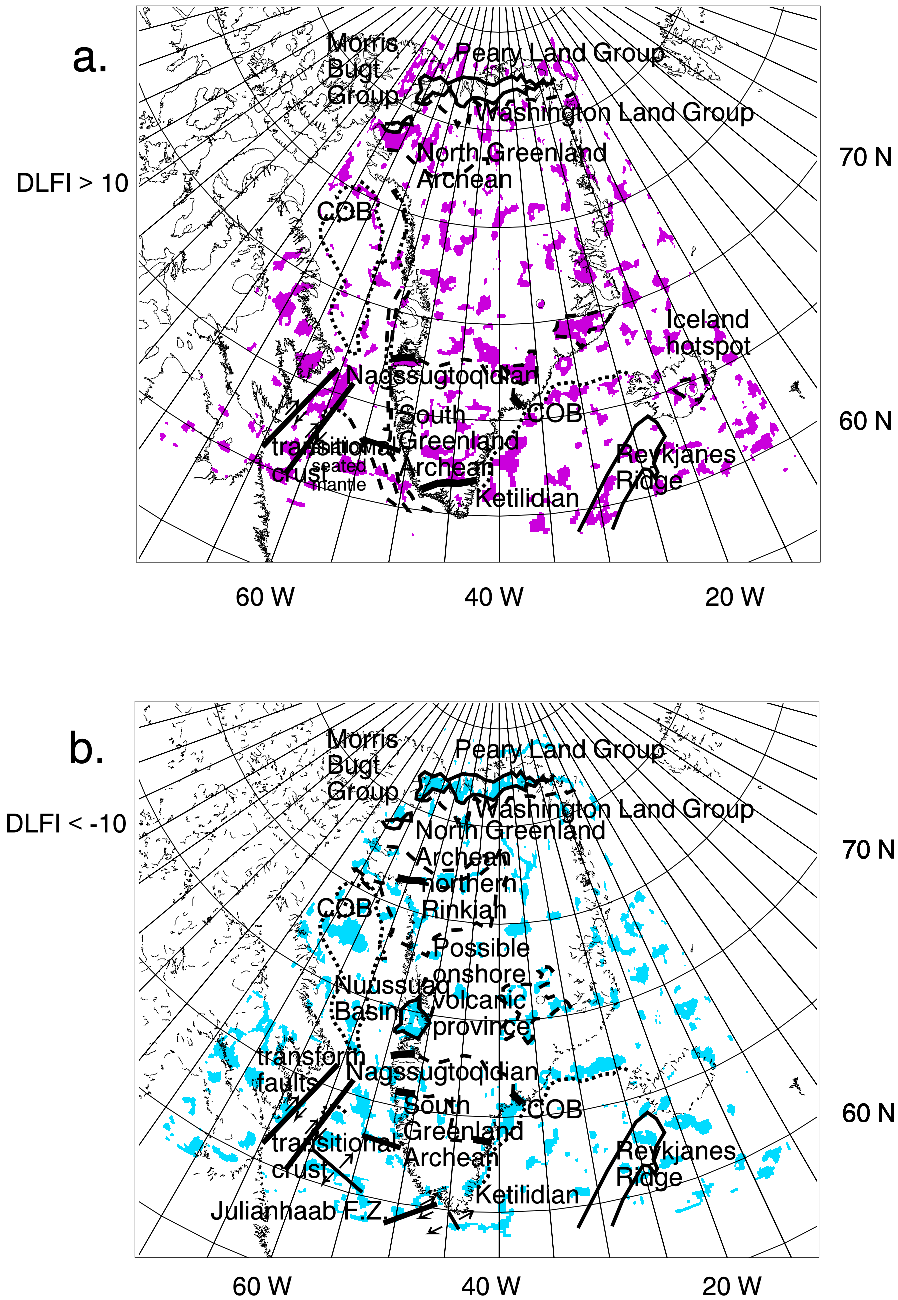

Figure 4.24: Negatively correlated gravity and magnetic features for the Greenland study area in a Lambert Equal-Area Azimuthal Projection centered on 40° W. Noted features are discussed in the text. **a**) The stronger FAGA peak-to-MA trough correlations given by DLFI>ASD(=10). **b**) The stronger FAGA trough-to-MA peak correlations given by DLFI<-ASD.

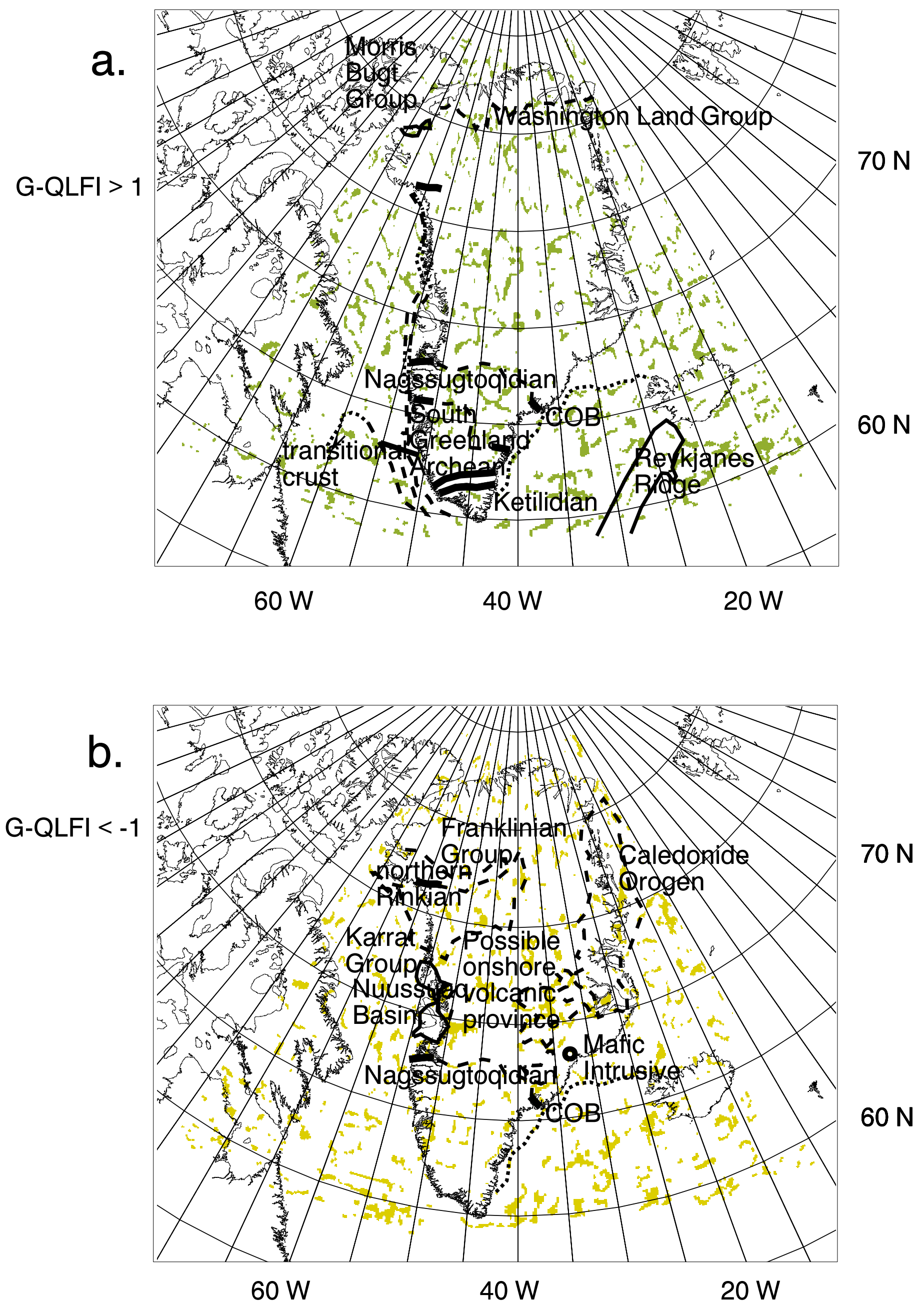

Figure 4.25: Gravity-quotient local favorability indices (G-QLFI) greater than 1 in a Lambert Equal-Area Azimuthal Projection centered on 40°W. G-QLFI were generated by dividing Figure 4.20 by the absolute value of Figure 4.19. Noted Features are discussed in the text. **a**) Gravity maxima with null correlated magnetic anomalies. **b**) Gravity minima with null correlated magnetic anomalies.

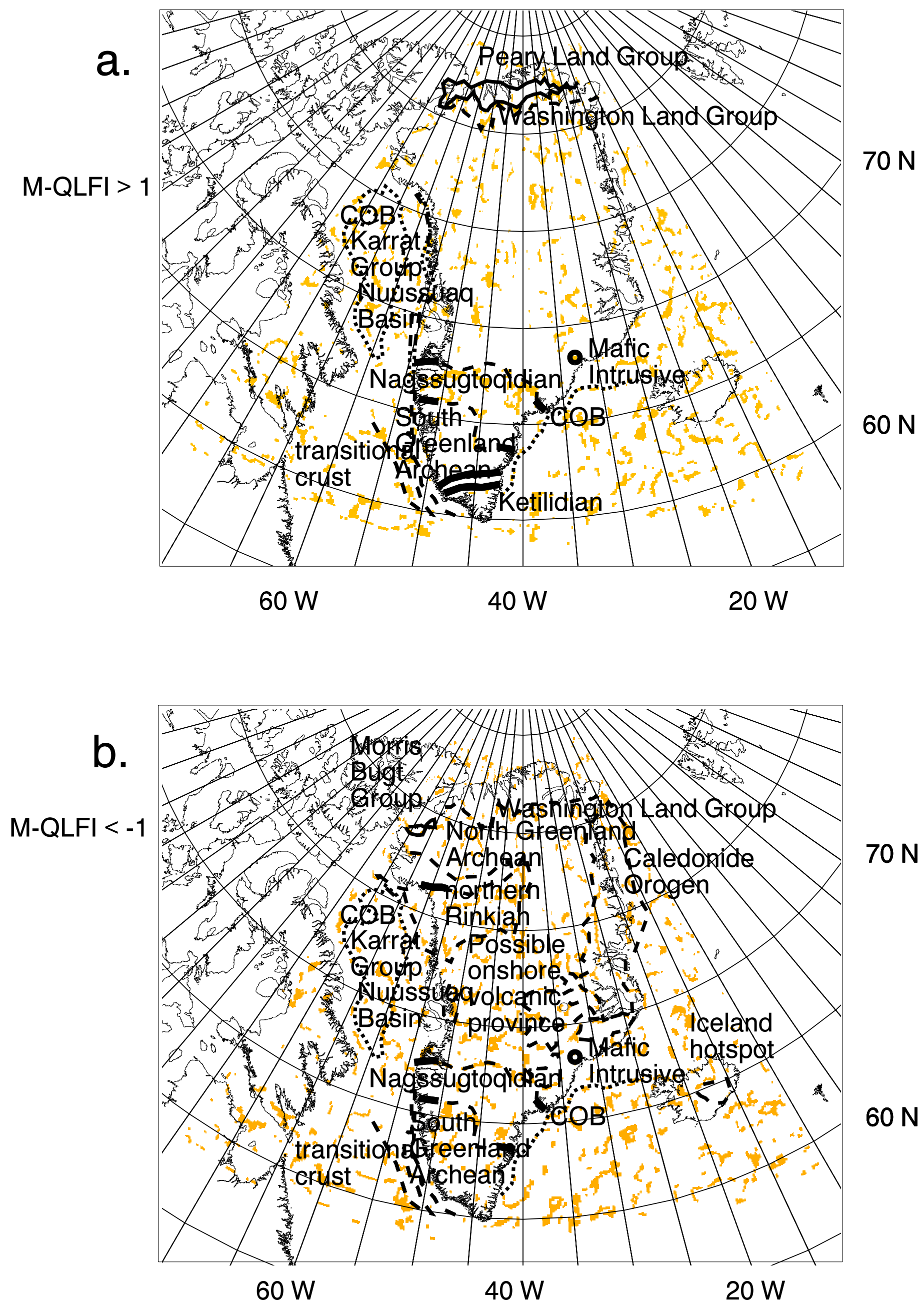

Figure 4.26: Magnetic-quotient local favorability indices (M-QLFI) greater than 1 in a Lambert Equal-Area Azimuthal Projection centered on 40° W. M-QLFI were generated by dividing Figure 4.19 by the absolute value of Figure 4.20. Noted Features are discussed in the text. **a**) Magnetic maxima with null correlated gravity anomalies. **b**) Magnetic minima with null correlated gravity anomalies.

northeastern edges of that province are also marked by sharp transitions to correlative negative density and magnetic susceptibility contrasts as shown in Figure 4.22.b, while the central border area is marked by an inverse contrast with positive density and negative magnetic susceptibility shown in Figure 4.24.a. Although no significant anomaly features are noted for the Nagssugtoqidian Province in Figures 4.22.b or 4.24.a, these figures do show the immediately adjacent regions and delineate where the Nagssugtoqidian Province ends.

Negative FAGA and positive MA (Figure 4.24.b characterize the rocks within the Peary Land Group, while both positive (Figure 4.22.a) and negative (Figure 4.22.b) FAGA and MA define the edge of this group. The composite of all boundaries determined from Figures 4.22, 4.24, 4.25, and 4.26 is shown in Figure 4.27.

An exhaustive list of all features within Greenland is not intended in this study, merely a validation of the process and a regional determination of the density and magnetic susceptibility contrasts for rocks located along the southwestern Greenland margin, which may provide insight into the possible tectonic development of Greenland and the Arctic.

The crustal region containing deep roots approximately 250 km off the southwestern Greenland coast is noted in Figures 4.22.a, 4.25.a, 4.26.a, and 4.26.b. The presence of features with intermediate to high positive density and magnetic susceptibility contrasts within the root structure is suggested by correlative anomalies in Figures 4.22.a, 4.25.a, and 4.26.a. To the west, the region is characterized by negative MA and null FAGA in Figure 4.26.b, which indicates a transition a region containing lower magnetic susceptibilities. To the east, the region is characterized by positive FAGA and negative MA in Figure 4.24.a and also suggests a transition to a region containing lower magnetic susceptibility contrasts.

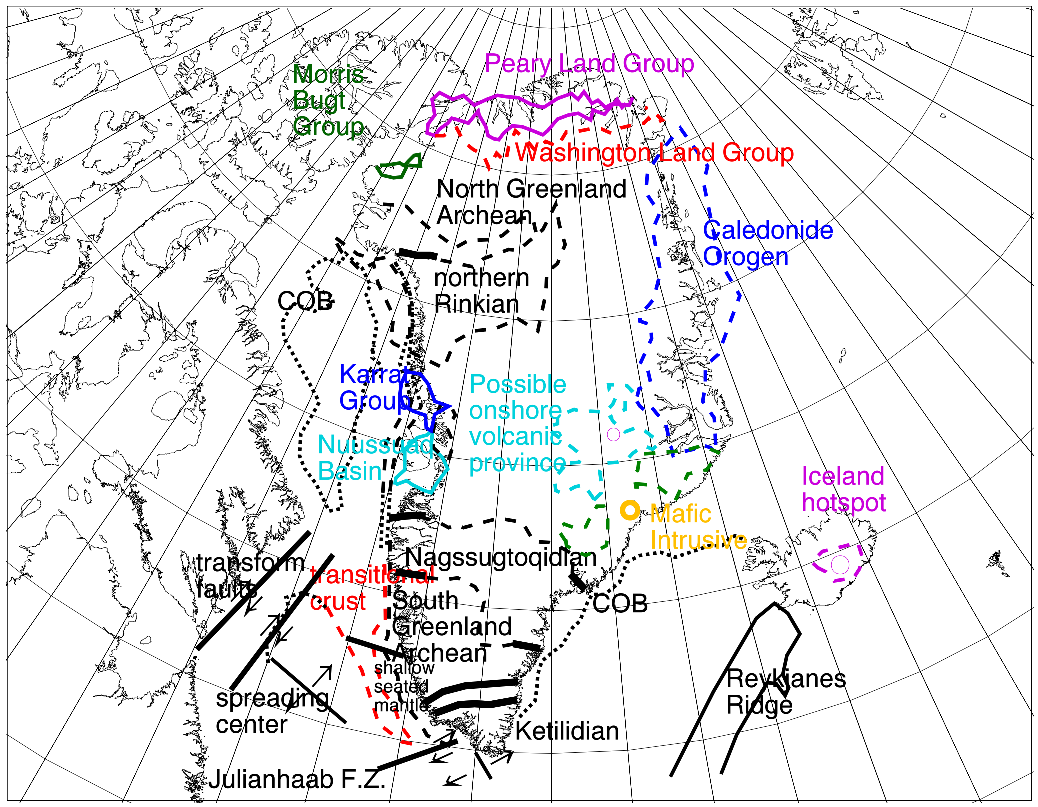

Figure 4.27: Composite geology and structural map of Greenland in a Lambert Equal-Area Azimuthal Projection centered on 40° W. These features were compiled from Figures 4.22, 4.24, 4.25, 4.26, and from the structure implied in Figure 4.1.

This region was interpreted as possible transitional crust with oceanic crust to the west and rifted continental crust above a shallow seated mantle to the east [Chapter 3; Chian and Louden, 1994; Chian et al., 1995a; 1995b]. The density and magnetic susceptibilities suggested here by the LFI-analysis supported this interpretation as did the structures implied by the gravity-derived Moho depth model (Figure 4.1) [Chapter 3].

One other result for discussion relates to the regional FAGA maxima shown in Figure 4.10. Mantle processes appear to be broadly related to anomalies that have wavelengths between 400 and 1000 km in the Earth's gravity field [Anderson, 1998]. These components of MC-TDFAGA that are shown in Figure 4.10 tend to exhibit relatively prominent affinities with several hotspot tracks that have been inferred for the Greenland study area.

For example, well defined MC-TDFAGA maxima are observed for Iceland that extend NE towards Greenland along the hotspot track. Regional gravity maxima also are affiliated with the Jan Mayan Island hotspot and Greenland coast. Other maxima appear to reflect the effects of the Yermak Plateau hotspot track.

Assuming that these regional gravity maxima actually indicate the trail of the hotspots, then it may be possible to generate a better reconstruction of plate movements over hotspots. Evidence for the passage of the Iceland hotspot under Greenland is suggested by the mafic intrusive region [Escher and Pulvertaft, 1995] noted in coastal eastern Greenland in Figure 4.26 and by a similar feature in east-central Greenland noted in Figures 4.24.a. This inland feature is associated with positive FAGA and negative MA. It is surrounded by a region of negative MA shown in Figures 4.26.b. These features occur in a region that the Iceland plumehead passed beneath and may represent the possible effects due to regional volcanism.

4.8 Conclusions

A new approach has been developed for the combined use of free-air gravity (FAGA) and magnetic (MA) anomalies for crustal studies in the Greenland region. This procedure offers a possible means of determining geologic information on Greenland where little information is available due to limited outcrops and extensive glacial and marine cover. The procedure determined gravity effects of the Earth's terrain to separate FAGA into terrain-correlated (TCFAGA) and -decorrelated (TDFAGA) components.

TDFAGA were assumed to reflect crustal and subcrustal density variations. FAGA determined from the EGM96 spherical harmonic coefficients were used to separate the components (MC-TDFAGA) related possibly to mantle and core density variations from those (IC-TDFAGA) possibly related to intracrustal density variations. Similarly, components of MA related to crustal thickness variations were removed for the components (IC-RTPMA) that were assumed to arise from intracrustal sources.

The MA were assumed to be related to variations of crustal thickness, crustal composition, and other processes. By determining those components most related to crustal thickness variations as inferred from a gravity-derived Moho depth model, the IC-RTPMA were separated for comparison with IC-TDFAGA using spectral correlation theory to identify correlative anomaly fields. The geologic significance of these correlative anomalies was considered, in particular for southwestern Greenland.

The poorly understood crust off southwest Greenland was found to be structurally and compositionally more characteristic of continental or transitional crust. Correlative gravity and magnetic maxima suggest that the near-shore zone may involve relatively shallow mantle. These results are also supported by structure determined from a gravity-derived Moho model [Chapter 3], available geologic data [Escher and

Pulvertaft, 1995], and seismic surveys [Chian and Louden, 1994; Chian et al., 1995a; 1995b].

A processing step for the TDFAGA data in this analysis separated possible mantle and core components (MC-TDFAGA). Maxima in these anomalies show strong affinities to hotspot trails and may offer a means of determining hotspot trails under continents. Additional evidence for the hotspots passage along this possible trail is seen by evidence for mafic intrusives in coastal Greenland observed in both the potential field data and in available geologic maps [Escher and Pulvertaft, 1995]. Further along this possible trail are correlative gravity minima and magnetic maxima that suggest the possibility of extensive distributions of volcanic rocks beneath the glacial cover of east-central Greenland.